STRESS-DEFORMATION PREDICTION IN CEMENT-TREATED SOIL PAVEMENTS

Mian-Chang Wang, University of Rhode Island; and
James K. Mitchell, Institute of Transportation and Traffic Engineering, University of California, Berkeley

The applicability of elastic-layer theory and the finite-element method for the prediction of stresses and deflections in cement-stabilized soil pavements under repeated plate loads has been found to be good. Two pavement test sections, each 8-in. thick and 20 by 20 ft in plan were constructed by using a cement-treated silty clay overlying a clay subgrade. Pavement 1 contained 3 percent cement, and pavement 2 contained 6 percent cement. Instrumentation was developed and installed in the pavement that allowed measurement of vertical deflections both at the pavement surface and near the bottom of the stabilized layer, compressive stress at the top of the subgrade, and radial strain at the bottom of the stabilized layer. Characterization of material properties for use in analysis was done by using the results of strength and repeated load compression and flexure tests on undisturbed samples taken from the test sections. Because the results of this investigation demonstrate that stresses and strains in cement-stabilized soil pavements can be predicted successfully by using existing theory, a basis for pavement thickness design may be possible that limits critical stresses and strains within the pavement and subgrade to acceptable values.

•THE RESULTS of a survey recently completed by Fohs and Kinter (9) indicate that the current annual usage of cement-stabilized material in pavement structures in the United States averages about 50 million sq yd. This corresponds to approximately 3,500 miles of 24-ft wide roadway—a not inconsiderable amount of construction.

In spite of this large volume and the associated construction costs, most agencies base the thickness and quality design of cement-stabilized layers on empirical rules. Although it is likely that some degree of empiricism, or perhaps more properly reasoned adjustment of the design thickness, will always be required to account for factors not readily analyzable, improved methods of thickness design are needed.

The steps required for the development of an improved design technique have been listed (2) as follows:

1. Identification of loading and environmental conditions,
2. Characterization of material properties,
3. Establishment of failure criteria,
4. Stress and deformation analysis of a system representative of the pavement structure, and
5. Performance studies in the field for verification and modification of the proposed method.

A number of studies have provided information relative to steps 2 and 3, e.g., those by Felt and Abrams (8), Abrams (1), Bofinger (4), Shen and Mitchell (18), and Larsen and Nussbaum (13). Studies of field performance have been reported by Childs and

Sponsored by Committee on Soil-Portland Cement Stabilization and presented at the 50th Annual Meeting.

Nussbaum (5), Highway Research Board (11), Larsen (12), Mitchell and Freitag (15), and Nussbaum and Larsen (17). Mitchell and Shen (16) have considered how a stress and deformation analysis (step 4) might be used as a basis for soil-cement thickness design. Larsen, Nussbaum, and Colley (14) have combined considerations of the load-deflection and fatigue behavior of soil-cement into a tentative design method for soil-cement pavements.

A field test program designed to provide information on the behavior of slabs of cement-stabilized soil under static and repeated loading has been completed. The test sections provided information useful for steps 2, 3, and 5 of the design process. Of particular interest in these tests was the direct measurement of stresses and strains at the bottom of the treated layer.

Studies have been made of the applicability of existing theory for the prediction of stresses and deflections in the pavement structure (step 4), and it is the purpose of this paper to describe these analyses and to compare prediction and observation.

TEST PAVEMENTS

Two test pavements each 20 by 20 ft in plan were constructed at the Richmond Field Station, University of California. The test pavements were essentially 2-layer systems each having an 8-in. thick cement-stabilized soil layer overlying the natural subgrade. A silty-clay soil was used in the stabilized layer, and the subgrade was a yellow clay. Classification properties of these soils are given in Table 1. The natural subgrade had a fairly uniform moisture content of about 20 percent and an average field CBR of about 8 to a depth at least 5 ft below the ground surface. Pavement 1 was constructed by using 3 percent cement by weight, and pavement 2 contained 6 percent cement. Construction details are presented by Wang, Mitchell, and Monismith (19).

Each test pavement had 9 different locations for repeated plate load tests. These 9 test sites were so distributed that the minimum spacing between the center of each site was 6 ft and the minimum distance from the center of any test site to the sides of the pavement was 4 ft as shown in Figure 1. These spacings, as verified from the test results, were sufficient to minimize the effects of pavement edges on the field performance as well as the repeated load tests on the soil properties at adjacent test sites.

LOADING FACILITIES AND INSTRUMENTATION

An 11,000-lb capacity loading piston actuated by compressed air was used to apply repeated loads at a frequency of 20 cycles/min and a duration of 0.1 sec. Reaction was provided by a beam that was fastened perpendicularly to the chassis at the end of a truck that carried 4 concrete blocks as reaction weight. During the test, the reaction beam was jacked up and supported by 2 wooden blocks. Photographs of the test setup are shown in Figures 2 and 3.

TABLE 1

SOIL CLASSIFICATION DATA

Property	RFS Silty Clay in Stabilized Layer	RFS Clay in Subgrade
Liquid limit, percent	29.2	56.3
Plastic limit, percent	19.4	22.6
Plastic index, percent	9.8	33.7
Specific gravity	2.65	2.66
Organic content, percent	2.5	1.3
Mineral composition of -2 μ fraction	Illite and montmorillonite	
Classification		
AASHO system	A-4	A-7
Unified system	CL	CH
Textural system	Clay loam	Clay

At each test site, 3 plates of different sizes were used, and a series of pressure intensities was applied to each plate in the sequence given in Table 2. In all cases the smallest plate was tested first, and the applied pressures were increased from the smallest value in order to minimize the prestress effects.

A stress gage of the diaphragm type was used for measuring vertical compressive stress at the top of the subgrade, a strain gage was used for measuring radial strain at the base of the cement-stabilizer layer, and dial gages were used to measure deflection at the top of the subgrade and at the surface of the pavement. The stress and strain gages were installed at the time of construction of the test pavements.

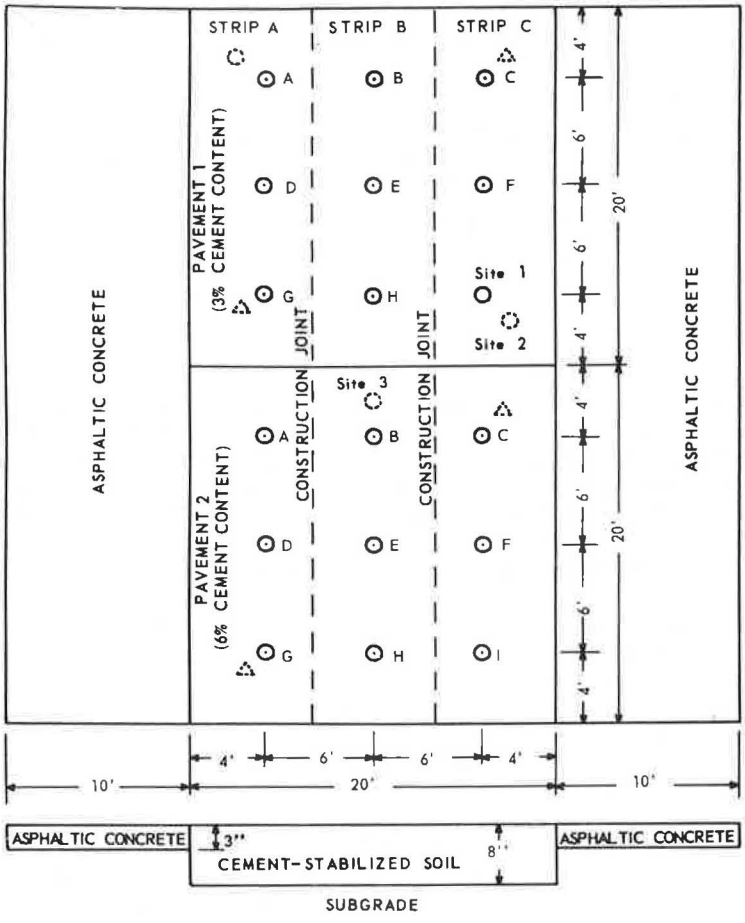

Figure 1. General layout of prototype pavements.

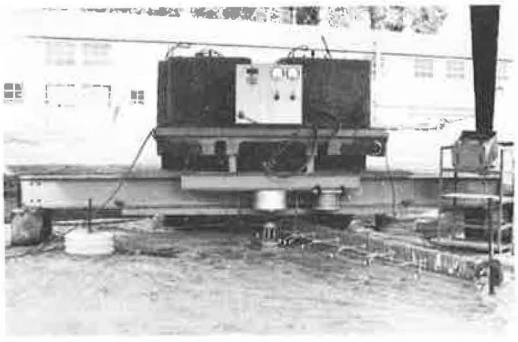

Figure 2. General view of repeated plate load test.

Figure 3. Close-up view of loading plate and gage system.

Gages were installed on the top of the subgrade at both sides of the center of loading plate in such positions that the center of the stress gage was 3 in. away from the center of the loading plate, whereas the central point of the strain gage was 2 in. off the centerline of the loading plate (Fig. 4). This arrangement was adopted to prevent the stress gage response from being affected by stress concentrations due to the presence of the strain gage and a $^{7}/_{16}$-in. diameter vertical hole used for measuring vertical deflection at the top of the subgrade. The effect of the release of vertical pressure at the bottom of the $^{7}/_{16}$-in. hole on the vertical stress acting on the stress gage was studied by using the approach suggested by Geddes (10), and it was found that the effect of pressure relief at a point 2 in. away and 1.5 in. from the bottom of the $^{7}/_{16}$-in. hole was insignificant.

TABLE 2

PLATE SIZES AND PRESSURE INTENSITIES USED IN REPEATED PLATE LOAD TESTS

Layer	Plate Diameter (in.)	Pressure Intensities (psi)
Subgrade	18	1, 2, 4, 8, 12
	24	1, 2, 3, 5, 8
	30	0.5, 1, 2, 3, 5
Pavements	8	10, 20, 40, 70, 100
	12	10, 20, 30, 40, 60
	18	5, 10, 15, 20, 30

Some aspects of the design, construction, and calibration of the stress and strain gages are given in the Appendix, and complete details are given by Wang, Mitchell, and Monismith (19). The stress gage was made of aluminum alloy casing with a foil type of strain gage cemented on the inner face of a diaphragm. Performance of the stress gages in pavement 1 was very satisfactory. The gages in pavement 2, however, did not perform as well, probably because the outputs of the gages in this pavement were too small to be read accurately.

The strain gage was composed of two $1^{1}/_{2}$ by $^{3}/_{4}$ by $^{1}/_{8}$ in. aluminum end plates used as reference points and a single linear variable differential transformer (LVDT) for measuring change in spacing between them.

The 0.001-in. dial gages used to measure deflections were attached to a 3 in. by 7 in. by 20 ft reference beam that was, in turn, anchored at points 10 ft away from the center of the test site and was stiffened laterally to prevent sway. For measuring deflection of the subgrade at a point under the center of the loading plate, a $^{7}/_{16}$-in. diameter hole was drilled to a depth of 1.5 in. above the top of the subgrade. A $^{1}/_{8}$-in. adjustable vertical rod was fastened to the bottom of the hole with Type III portland cement

With the aid of this test set up and instrumentation, it was possible to measure (as a function of plate size, applied pressure, and curing time for each pavement) the following quantities after any desired number of load repetitions:

1. Vertical deflections at the surface,
2. Vertical stress at the bottom of the stabilized layer (top of subgrade),
3. Radial strain at the bottom of the stabilized layer, and
4. Vertical deflection near the bottom of the stabilized layer.

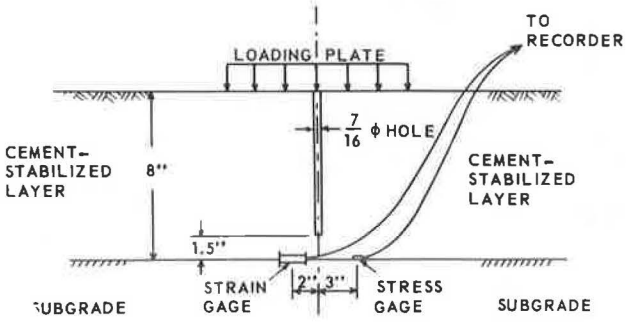

Figure 4. Schematic view of gage positions.

It was found that for any plate size, plate pressure, and curing time the stress and deflection responses were essentially constant after about 300 load repetitions. Thus, values reported subsequently are those corresponding to 300 load repetitions.

MATERIALS CHARACTERIZATION

In order to investigate the suitability of theory for prediction of stresses and deflections, certain material properties must be known or assumed for

each layer, e.g., strength, modulus, and Poisson's ratio. Both undisturbed specimens taken directly from the test pavement sections and specimens compacted in the laboratory were tested to provide this information. A summary of the test results is given in Table 3.

The unconfined compressive strength of the undisturbed specimens was about 50 percent of that of the laboratory-compacted specimens; the ratio of the resilient modulus in compression for undisturbed specimens to that for laboratory-compacted specimens was approximately 40 percent. The ratios for both flexural strength and resilient modulus in flexure are 69 percent and 57 percent respectively. It should be noted that the results for flexural tests were measured from only 4 undisturbed beam specimens. Difficulty in sampling precluded obtaining more beam specimens.

The large difference between strengths of field and laboratory-compacted samples were somewhat surprising because the field-mixing procedures were thought to be quite good. Nonetheless, the differences were significant, and the results point to a problem that remains largely unsolved when dealing with stabilized soils: how to predict properties of the stabilized layer in the field from the results of laboratory tests prior to construction. Because of these large differences, only the values obtained from the undisturbed specimens were used for the analyses described in the next section.

Although strength and modulus increased with increase in curing time and cement content for both compression and flexural loading conditions, the strain at failure under static load was constant regardless of sample age and cement content.

The resilient modulus in flexure was sensibly independent of the repeated stress level. The resilient modulus in compression, however, depended on both confining pressure and repeated stress according to the following expression:

$$M_R = K_1(K_2 - \log_e \sigma_d)I_1^{K_3} \quad (1)$$

where K_1, K_2, and K_3 are constants, σ_d is deviator stress, and I_1 is the first stress invariant.

A linear relationship between unconfined compressive strength and flexural strength was found; the modulus of rupture was about 20 to 35 percent of the unconfined compressive strength.

Although the modulus of resilient deformation in compression of the cement-stabilized soil could be represented by Eq. 1, the subgrade modulus of resilient deformation in compression was represented by an idealized bilinear function as shown in Figure 5 and expressed in the following form:

$$M_R = K_1 + (K_2 - \sigma_d)K_3, \text{ for } \sigma_d < K_2 \quad (2)$$

or

$$M_R = K_1 + (\sigma_d - K_2)K_4, \text{ for } \sigma_d > K_2 \quad (3)$$

TABLE 3

STRENGTH AND RESILIENT MODULI FOR UNDISTURBED AND LABORATORY-COMPACTED SPECIMENS

Specimens	Cement (percent)	Strengths (psi)		Resilient Moduli (10^3 psi)	
		Unconfined Compressive	Flexural	Compression	Flexure
Laboratory-compacted	3	60 - 110	15 - 40	40 - 150	60 - 180
	6	110 - 250	55 - 95	160 - 320	130 - 440
Undisturbed	3	20 - 50	—	10 - 95	—
	6	60 - 150	65	20 - 170	250
Ratio of undisturbed to laboratory-compacted	3	0.33 - 0.45	—	0.25 - 0.63	—
	6	0.55 - 0.60	0.69	0.13 - 0.53	0.57

Note: Ranges in values reflect influences of variations in curing period, density, and moisture content.

Development of these equations is given in an earlier report (19).

A summary of the values of properties and coefficients derived from the test results for the different materials and different curing times that are needed for analysis of stresses and deflections is given in Table 4. The lower values of subgrade modulus associated with the longer curing periods given in Table 4 resulted from an increase in subgrade moisture content. Poisson's ratio for the subgrade material was taken as 0.50 for analysis by elastic theory, as 0.48 for finite-element analysis, and as 0.20 for the cement-stabilized soil (3). (0.50 would be a more correct value, but the finite-element program cannot handle a value of 0.50.)

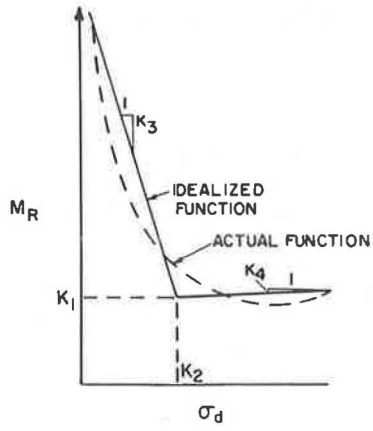

Figure 5. Characterization of subgrade modulus.

PREDICTION OF STRESSES AND DEFORMATIONS

Layered-elastic theory and finite-element analyses were used to predict surface deflections, radial strains at the base of the cement-stabilized layer, and vertical compressive stress on the top of subgrade near the centerline of the loading plate system for various curing times. The computed values were compared with the actual values measured in the repeated plate load tests.

Elastic-Layer Theory

Because the modulus of resilient deformation depends on the stresses, and the stresses and strains themselves are determined by the moduli values, a compatible solution requires successive approximations. Because the vertical and horizontal stresses induced in the prototype pavements by repeated plate loads may vary appreciably both vertically and horizontally, the resilient modulus within the pavement may vary considerably from place to place. Modulus variation in the vertical direction can be approximated by subdividing the pavement into several horizontal layers, each having a constant modulus throughout its thickness. Variations along a horizontal plane cannot be taken into account by using elastic-layer theory.

The behavior of the prototype pavements was analyzed by using successive approximations and an n-layer digital computer program developed by the Chevron Research Company (20). The pavement system was divided into 5 horizontal layers for analysis,

TABLE 4

PROPERTY VALUES USED FOR ANALYSES

Material	Curing Time (days)	Constants of Resilient Modulus in Compression (psi)				Resilient Modulus in Tension (10^3 psi)	Poisson's Ratio	Lateral Earth Pressure Coefficient
		K_1	K_2	K_3	K_4			
Soil stabilized with 3 percent cement	2	3,550	5.39	0.16	—	30.0	0.20	0.50
	23	3,550	4.52	0.44	—	45.0		
	100	3,550	4.12	0.65	—	60.0		
Soil stabilized with 6 percent cement	4	408	4.90	1.00	—	105.0		
	17	636	4.94	0.95	—	160.0		
	93	1,372	5.07	0.82	—	210.0		
Subgrade soils	2, 4, 23	14,500	4.5	1,000	-67.0	—	0.48	
	17	12,500	4.2	1,270	-100.0	—		
	93	3,800	2.4	2,250	-90.0	—		
	100	7,000	3.0	1,930	-85.0	—		

as shown in Figure 6, including 3 layers of 2-, 4-, and 2-in. thickness in the cement-stabilized soil section and 2 layers of 24-in. and infinite thickness in the subgrade. The surface load was assumed to be a uniformly distributed pressure on a flexible circular plate. The lateral earth pressure coefficient was assumed to be 0.50 throughout the entire pavement.

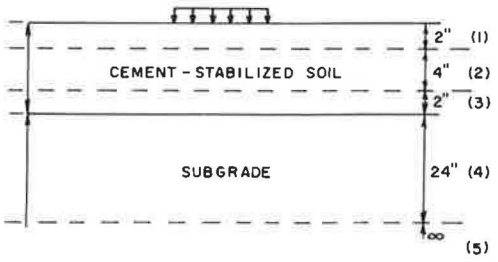

Figure 6. Five-layer representation of pavement section for analysis by elastic theory.

The procedure used for analysis was as follows:

1. Both the vertical and horizontal stresses at the mid-depth of each layer on the centerline of the loading plate system due to the surface load were estimated by using an approximate stress distribution (Boussinesq was used here);
2. The stresses induced by the weight of the pavement were added to the stresses estimated in step 1;
3. The approximate modulus of each layer in compression was estimated corresponding to the estimated stresses by using Eqs. 1 and 2, and the resilient modulus in flexure for tensile radial stresses was as given in Table 4;
4. The vertical stress and radial stress at the top and bottom of each layer were calculated by using the moduli determined in step 3, and the stresses at mid-depth of each layer were approximated by averaging;
5. The moduli corresponding to the stresses determined in step 4 were computed for each layer;
6. The moduli obtained in step 5 were compared with those estimated in step 3, and, if they were different, the whole procedure was repeated until the computed moduli were the same as the input values; and
7. When the estimated and computed moduli were in agreement, the deflections, strains, and stresses in the pavement were computed.

Finite-Element Analysis

The finite-element method of analysis has been proved to be an effective means for the analysis of axisymmetric solids by Clough and Rashid (6) and Wilson (21) and of pavement structures by Duncan et al. (7). In this method of analysis, the pavement structure is first idealized as an assemblage of a finite number of discrete structural elements interconnected at a finite number of joints or nodal points. The size of the elements are chosen to vary in accordance with the anticipated stress gradients. The finite elements for a pavement structure are actually complete rings in the horizontal direction, and the nodal points are in reality circular lines in plane view.

In the program used for this study, the pavement was divided into a series of quadrilaterals. Each quadrilateral was subsequently divided into 4 triangles by the computer program. Displacements were assumed to vary linearly within each triangle. The surface load was assumed to be a rigid circular plate load and to be applied stepwise so that the nonlinear stress-strain behavior and the modulus stress dependency of the cement-stabilized soil could be included in the analysis. Therefore, the accuracy of the solution is a function of the number of load increments used, with greater accuracy associated with smaller load increments.

The bottom boundary on which the nodal points are fixed was taken at a distance of about 50 radii beneath the pavement surface, and a vertical boundary on which the nodal points are constrained from moving radially was chosen at a distance of about 20 radii from the center of loading plate. A typical finite-element mesh for an 8-in. diameter loading plate is shown in Figure 7.

An element may be subjected to compression in one direction and tension in the other. For this case, the resilient modulus in compression was used only when the compressive strain was 5 times larger than the tensile strain because the ratio of failure strain

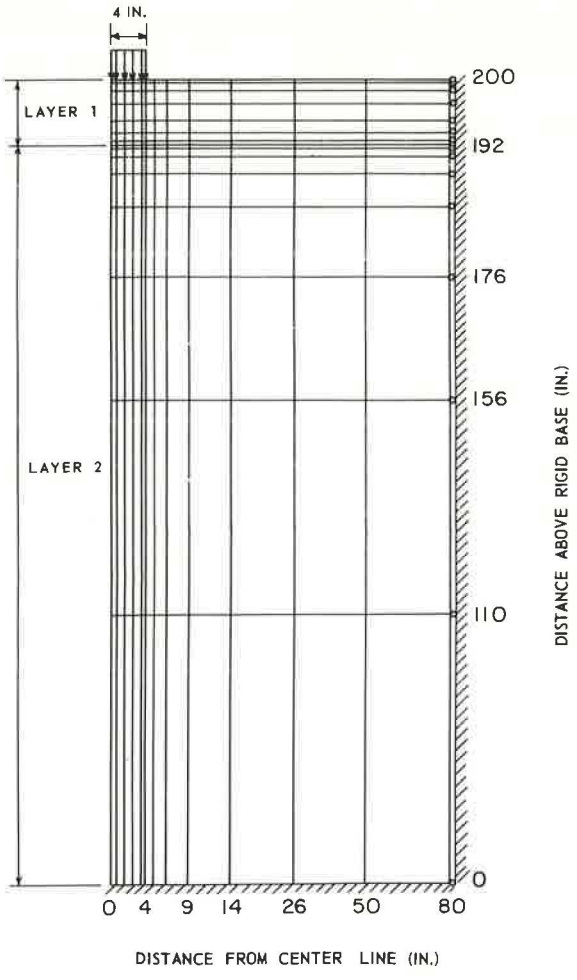

Figure 7. Finite-element configuration used for analysis of test pavements under 8-in. diameter plate.

in compression to that in tension equaled five. The element was considered to have failed when the shear strain induced from the applied load in the element reached the failure shear strain indicated by the laboratory test results. The resilient modulus of any failed element was assigned a small value (20 times less than the original value) for subsequent stress applications.

Resilient Deflections

Resilient deformations of pavement 1 cured for 2 days were predicted, and the results are shown in Figure 8. The resilient deformation of the pavement system agrees very well with the values computed by using elastic-layer theory. Shown in Figure 9 are the results of prediction of the resilient compressive strain in the cement-stabilized soil layer. It is seen that as the loading plate size increases the differences between predicted and measured values increase.

Although the finite-element analysis gives slightly lower predictions than the elastic-layer program, the agreement between the predicted and the actual deformations, especially at low plate pressures, is still quite good. Moreover, Figure 9 shows that the

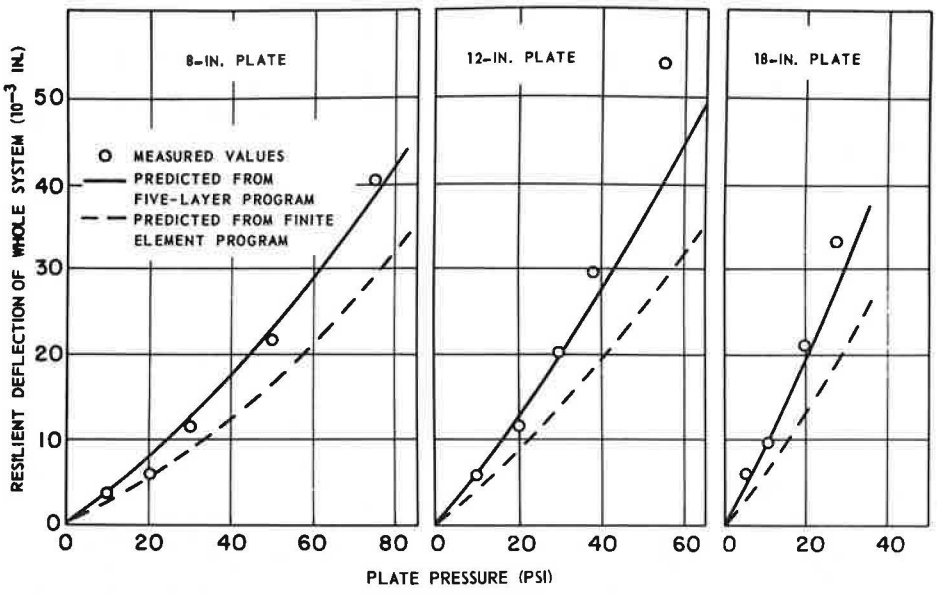

Figure 8. Resilient surface deflections in pavement 1 after 2-day curing.

finite-element analysis gives better predictions for the compressive strain in the stabilized layer than the elastic-layer program.

Figure 10 shows the predictions for surface deflection under a 12-in. diameter plate for pavement 1 after 23- and 100-day curing periods. The predictions, in general, are very satisfactory, and the analyses appear equally good for different curing times.

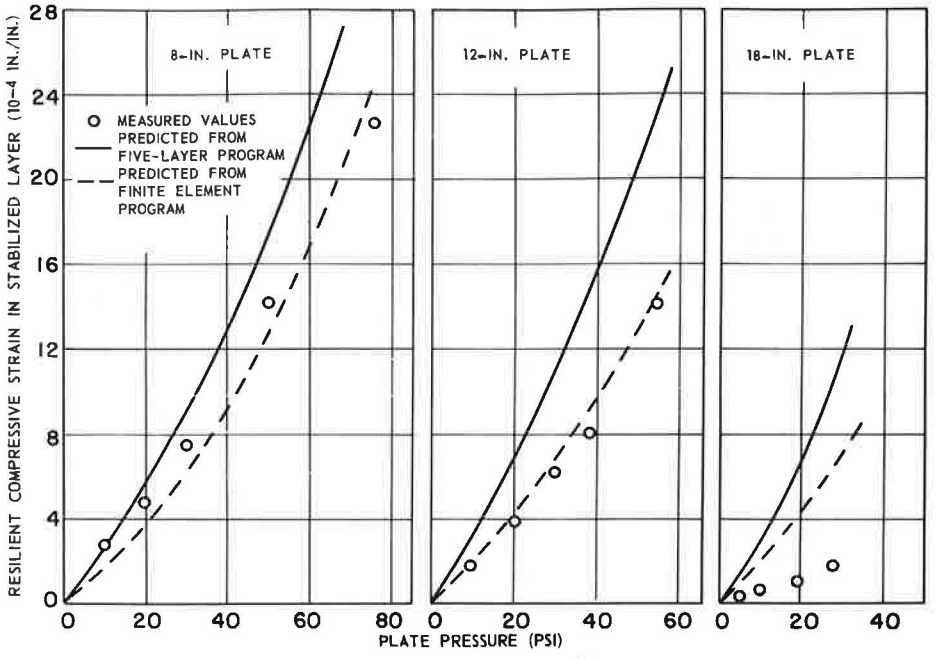

Figure 9. Resilient compressive strains in stabilized layer after 2-day curing.

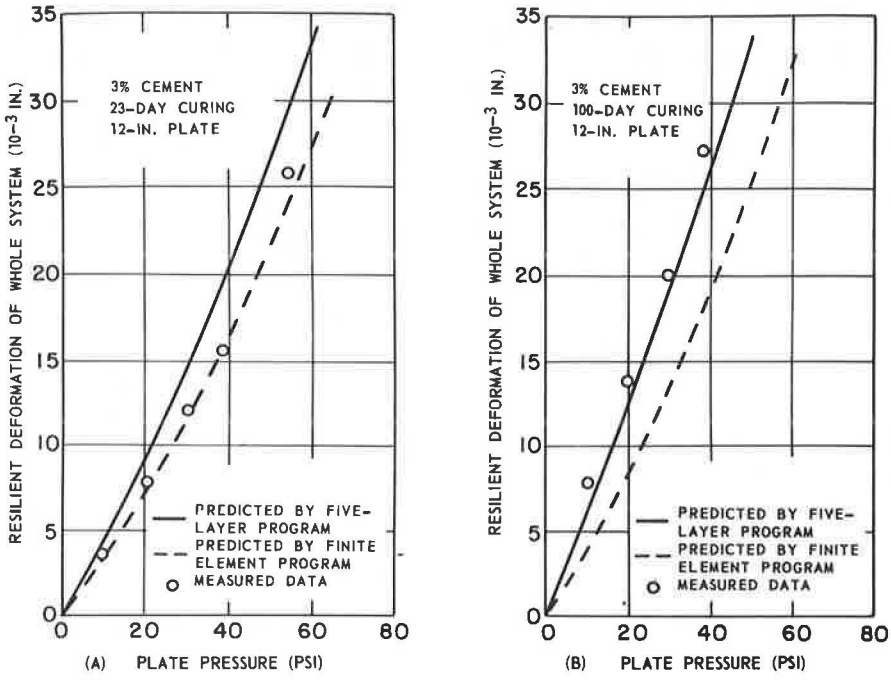

Figure 10. Resilient surface deflections in pavement 1 after 23-day and 100-day curing.

Figures 11 and 12 show the results of predictions for surface deflection pavement 1 because both theories predict values that are too high for all curing times. The results obtained from the finite-element analysis are in much better agreement with observation than those from elastic-layer theory, particularly at low plate pressure.

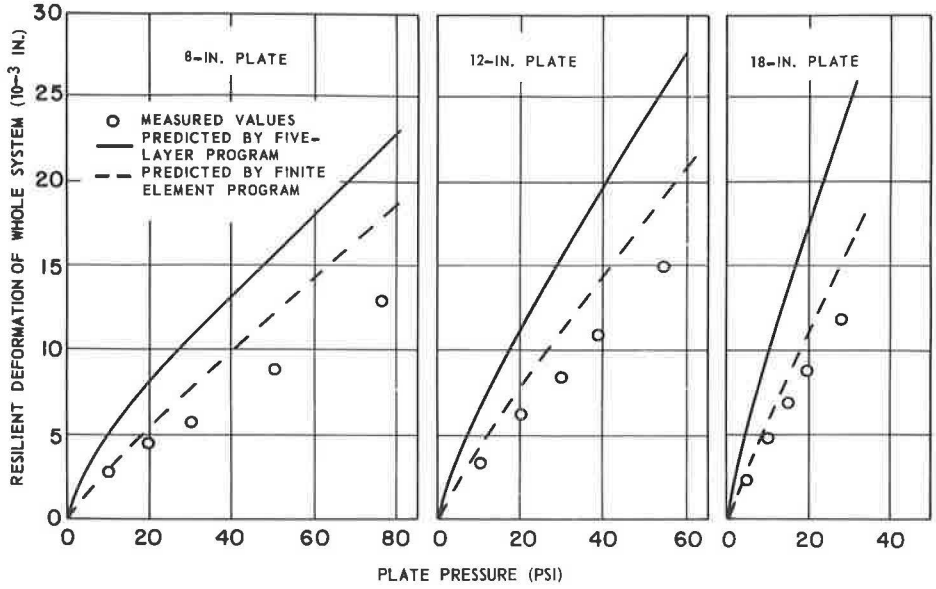

Figure 11. Resilient surface deflections in pavement 2 after 4-day curing.

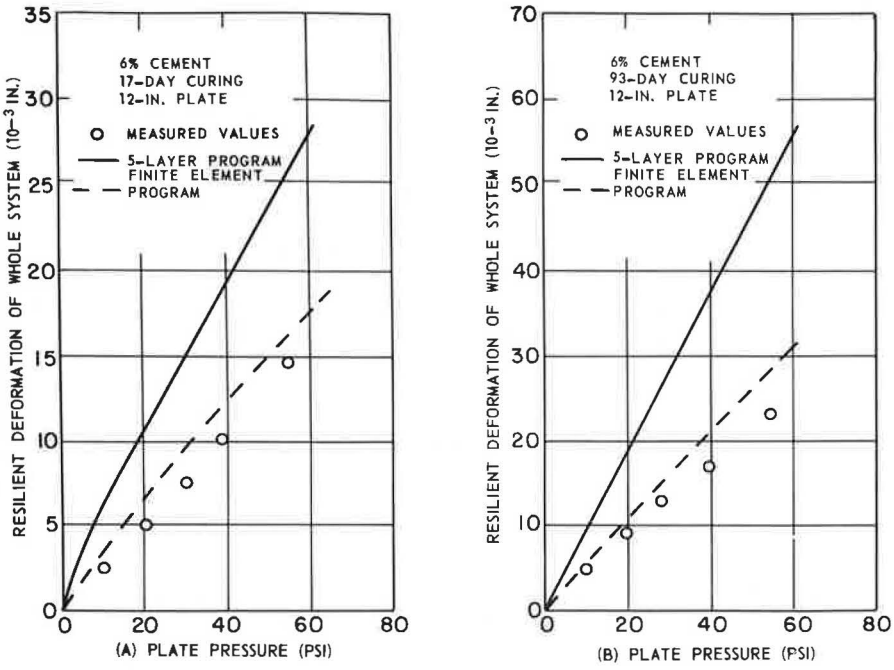

Figure 12. Resilient surface deflections in pavement 2 after 17-day and 93-day curing.

The results shown in Figures 8 through 12 indicate the following:

1. Elastic-layer theory gave better results than the finite-element analysis for the surface deflection in pavement 1. The finite-element analysis always underpredicted but still gave fairly reasonable results at low plate pressure.
2. For pavement 2, the finite-element analysis gave much better results than the elastic-layer theory but overpredicted somewhat.
3. Predictions were equally good at different curing times. This may imply that, although strength and modulus of the cement-stabilized soil increase with increase in curing time, the form of the stress-strain behavior did not vary significantly with time.
4. The finite-element analysis gave lower predictions than the elastic-layer theory; this behavior may be explained by the following. (a) The surface load was assumed to be a flexible circular load in the elastic-layer program, whereas it was assumed to be a rigid circular plate load in the finite-element program. Deflection under the rigid plate is constant throughout the whole contact area, whereas deflection under the flexible plate is a maximum at the center of the contact area. According to elastic theory for a homogeneous half space, the deflection under a rigid circular plate will be about 20 percent less than that under the center of a flexible loading of the same intensity. The assumption made in the finite-element analysis is more representative of the field test plate deflections than the assumption made in the elastic-layer program for the flexible loaded area. (b) In the elastic-layer program, the modulus of a layer is represented by the modulus corresponding to the stress acting at the intersection of the centerline of the loading plate and the mid-depth of the layer. Because the deviator stress on a horizontal layer is a maximum on the plate centerline, for a flexible surface loading, the corresponding modulus will be smaller than elsewhere. However, in the finite-element program, different moduli were used for different elements according to the state of stress acting on the elements. Therefore, the moduli values used in the elastic-layer program generally were less than those used in the finite-element program, leading to greater predicted deflections by the elastic-layer program than by the finite-element program.

Resilient Radial Strain at Bottom of Cement-Stabilized Soil Layer

Figures 13 and 14 show the results of predictions of resilient radial strain at the bottom of the stabilized layer for pavement 1 using both the elastic-layer program and the finite-element program. Both methods predicted very well at low plate pressure; but, as the plate pressure increased, the predicted values became smaller than the measured values. For longer curing times, both approaches gave better predictions at high plate pressure than at low plate pressure, and the finite-element program gave better predictions than the elastic-layer program.

The predictions made for pavement 2 are shown in Figures 15 and 16. The finite-element program predicted the values associated with a 4-day curing period very well. The elastic-layer program predicted slightly too high for all 3 plate sizes. For increased curing time, the predictions made from the finite-element program became poorer; on the other hand, the elastic-layer program predictions improved. The measured values are bracketed between the 2 predictions.

Vertical Compressive Stress on Top of Subgrade

The curves shown in Figure 17 compare measured and predicted values of vertical compressive stress on the top of the subgrade for pavement 1 after 2-day curing. Both the elastic-layer and the finite-element methods predicted well. However, as curing time increased, predicted values became larger than the measured values (Fig. 18). For longer curing times, the finite-element program gave better agreement than the elastic-layer program, but values were still overpredicted.

Both Figures 17 and 18 show that the finite-element program gave lower predictions than the elastic-layer program. The difference gradually decreased with increase in plate diameter. The reason for this may be as noted previously: Different assumptions for the surface load distribution were made in the elastic-layer program (assumed to be a flexible load) and in the finite-element program (assumed to be a rigid plate load). These different assumptions result in a difference in the distribution of contact pressure between the bottom of loading plate and the soil. The contact pressure under the flexible circular plate is constant over the loaded area, whereas the contact pressure

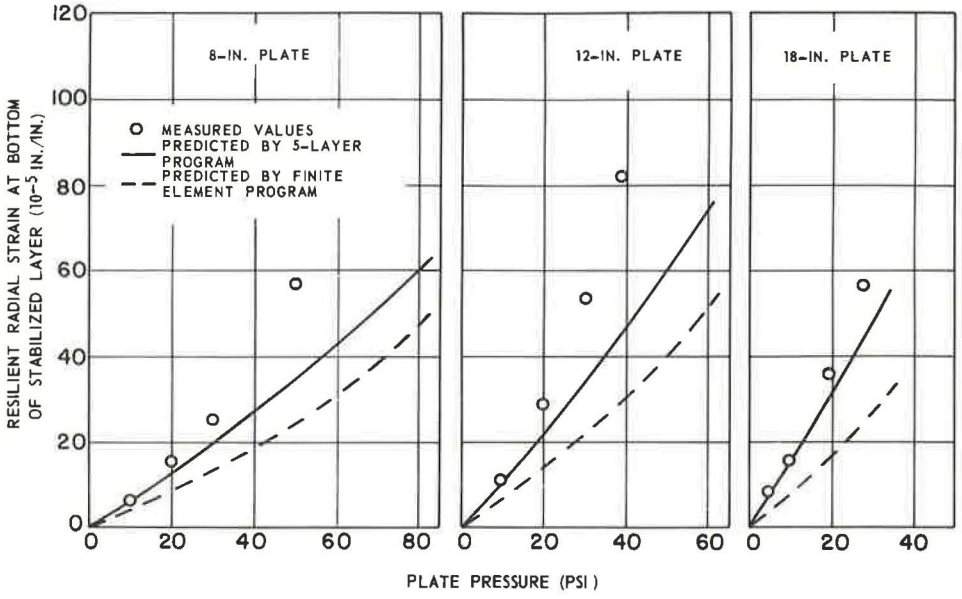

Figure 13. Resilient radial strains at bottom of stabilized layer in pavement 1 after 2-day curing.

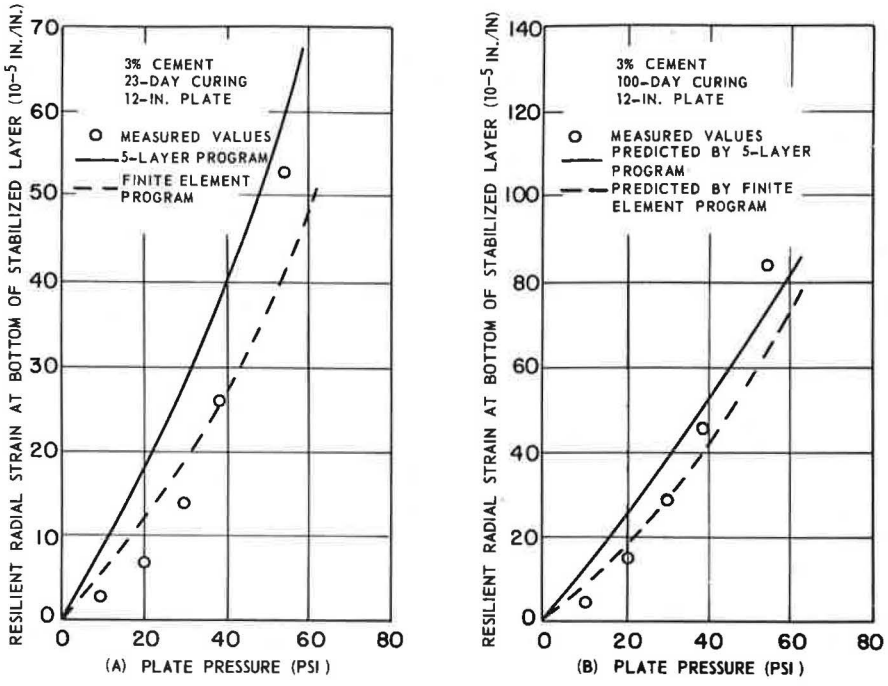

Figure 14. Resilient radial strains at bottom of stabilized layer in pavement 1 after 23-day and 100-day curing.

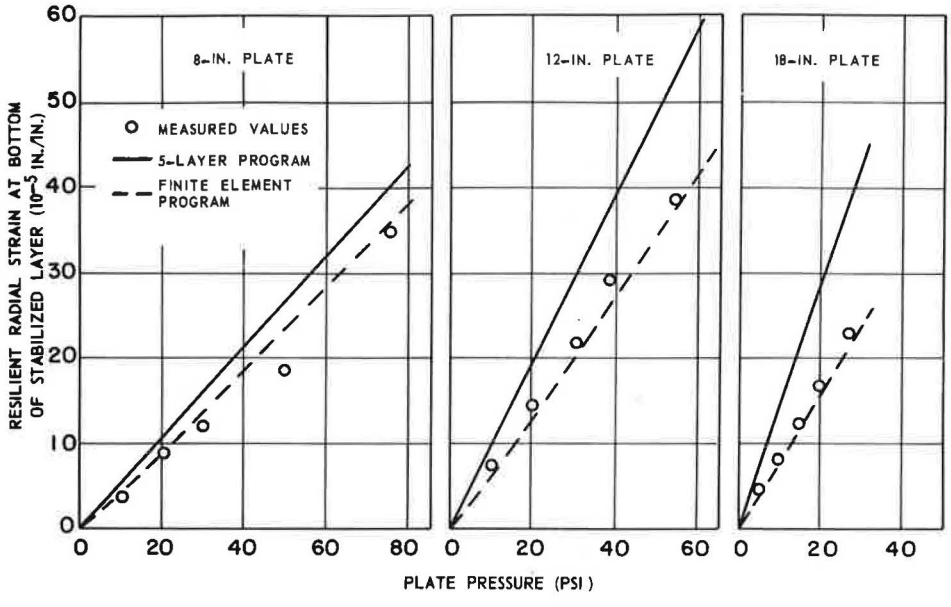

Figure 15. Resilient radial strains at bottom of stabilized layer in pavement 2 after 4-day curing.

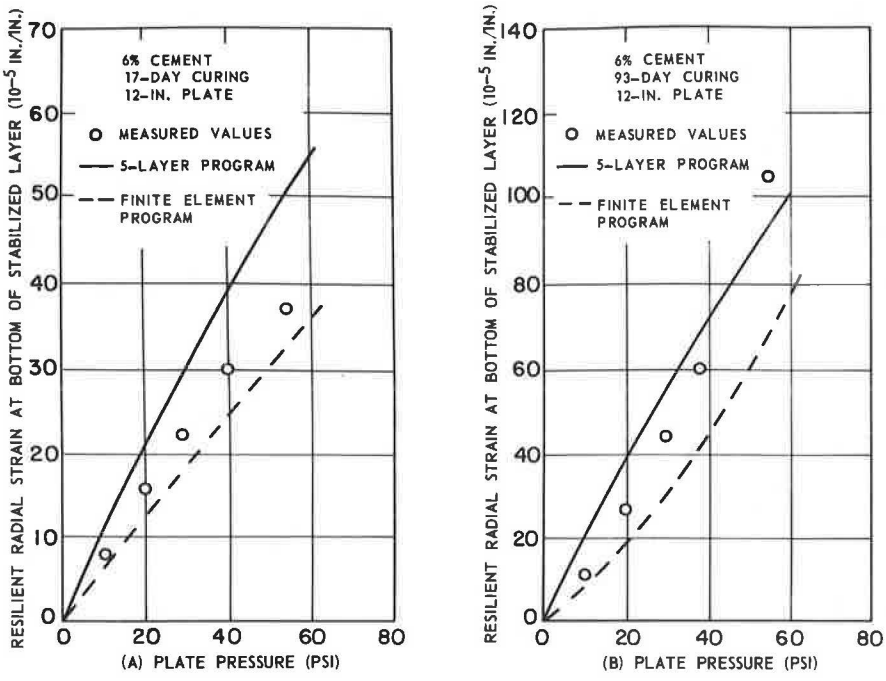

Figure 16. Resilient radial strains at bottom of stabilized layer in pavement 2 after 17-day and 93-day curing.

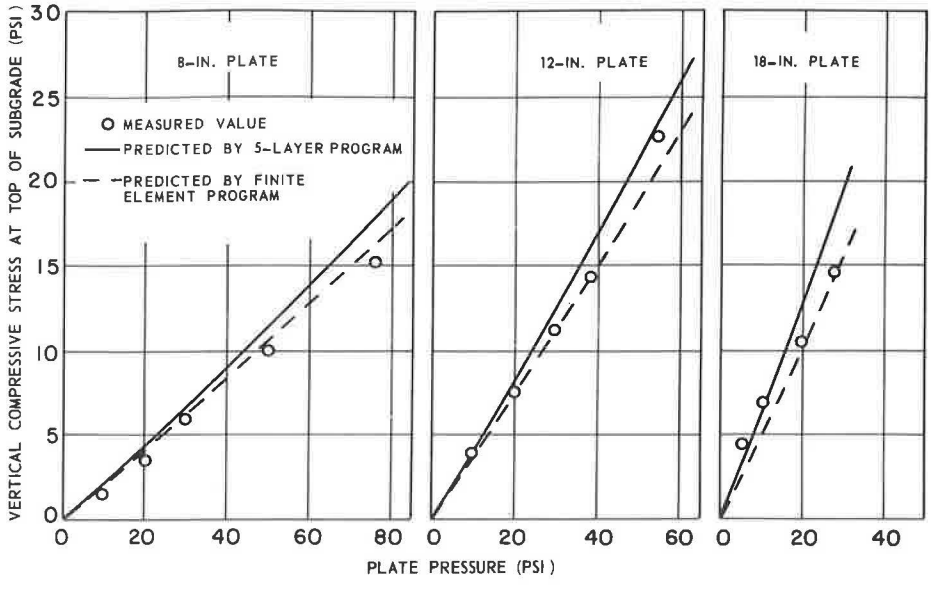

Figure 17. Vertical compressive stress at top of subgrade in pavement 1 after 2-day curing.

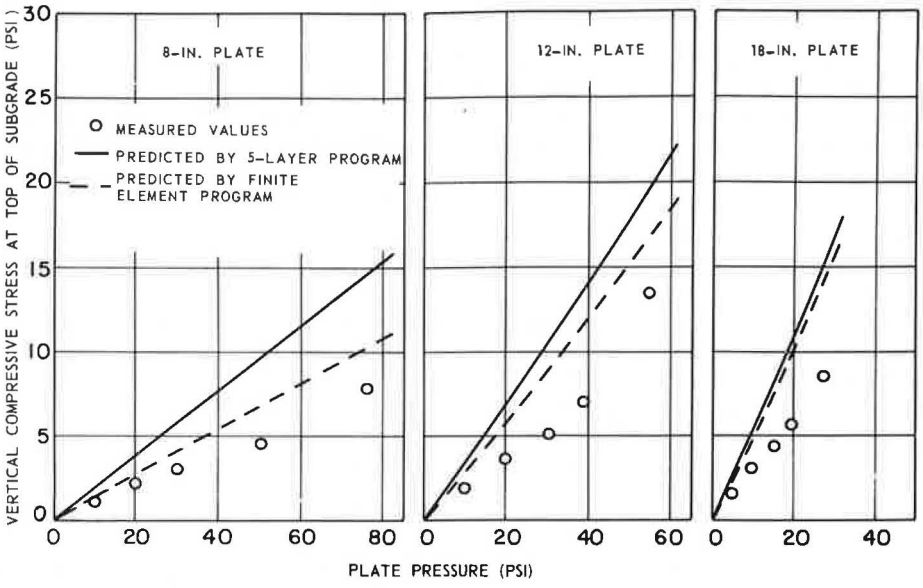

Figure 18. Vertical compressive stress at top of subgrade in pavement 1 after 23-day curing.

under a rigid plate is a maximum at the edges and a minimum at the center of the plate.

SUMMARY AND CONCLUSIONS

The primary purpose of this study was to investigate the applicability of available theories for predicting the induced stress and deflection response of 2 cement-stabilized soil pavement test sections to load. Both pavements consisted of a treated silty-clay soil layer, 8 in. thick overlying a clay subgrade. Pavement 1 contained 3 percent cement, whereas pavement 2 contained 6 percent cement. The study was divided into 3 phases: (a) field repeated plate load testing on 2 test pavements; (b) laboratory study of representative specimens, including laboratory-compacted and undisturbed specimens taken from the field, to determine appropriate material parameters to be used for prediction of stresses and deflections; and (c) prediction of stresses and deflections using available theories in conjunction with the appropriate measured values of material properties. This paper has been concerned mainly with the last phase.

Elastic-layer theory was found to predict quite well (a) surface deflection in pavement 1, (b) radial strain at the underside of the stabilized layer in pavement 1 at early stages of curing for low plate pressure, (c) radial strain in pavement 2 at later stages of curing, and (d) vertical stress in pavement 1 at early stages of curing.

Finite-element analysis predicted all field behavior under investigation reasonably well, except for the surface deflections in pavement 1 and the radial strains in pavement 1 at later stages of curing. Finite-element analysis always gave predictions lower than those given by elastic-layer theory. This may be attributed to the different assumptions for the plate flexibility.

The results of this investigation demonstrate that stresses and strains in cement-stabilized soil pavements can be predicted successfully by using elastic-layer theory and finite-element analysis together with material properties determined from laboratory repeated load tests on undisturbed specimens taken from the test pavements. Thus, a basis for pavement thickness design may be possible that limits critical stresses and strains within the pavement to acceptable values by using an approach similar to that suggested by Mitchell and Shen (16).

ACKNOWLEDGMENTS

The tests described and the resulting data presented here were obtained from research conducted for the U.S. Army Engineer Waterways Experiment Station, Vicksburg, Mississippi, and sponsored by the U.S. Army Materiel Command. The permission granted by the Chief of Engineers to publish this information is appreciated.

REFERENCES

1. Abrams, M. S. Laboratory and Field Tests of Granular Soil-Cement Mixtures for Base Courses. ASTM, Spec. Tech. Publication 254, 1959, pp. 229-243.
2. ASCE Committee on Structural Design of Roadways. Problems of Designing Roadway Structures. ASCE Transportation Eng. Jour., Vol. 95, No. TE2, May 1969, pp. 289-315.
3. Balmer, G. G. Shear Strength and Elastic Properties of Soil-Cement Mixtures Under Triaxial Loading. Proc. ASTM, Vol. 58, 1958, pp. 1187-1204.
4. Bofinger, H. E. The Fatigue Behavior of Soil-Cement. Jour. of Australian Road Research Board, Vol. 2, No. 4, June 1965, pp. 12-20.
5. Childs, L. D., and Nussbaum, P. J. Pressures at Foundation Soil Interfaces under Loaded Concrete and Soil-Cement Highway Slabs. Proc. ASTM, Vol. 62, 1962, pp. 1243-1263.
6. Clough, R. W., and Rashid, Y. Finite Element Analysis of Axi-Symmetric Solids. ASCE Jour. of Eng. Mechanics Div., Feb. 1965.
7. Duncan, J. M., Monismith, C. L., and Wilson, E. L. Finite Element Analyses of Pavements. Highway Research Record 228, 1968, pp. 18-33.
8. Felt, E. J., and Abrams, M. S. Strength and Elastic Properties of Compacted Soil-Cement Mixtures. ASTM, Spec. Tech. Publication 206, 1957, pp. 152-178.
9. Fohs, D. G., and Kinter, E. B. Current Practices of Soil-Cement Thickness Design. Paper presented at HRB 49th Annual Meeting, Jan. 1970.
10. Geddes, J. D. Stresses in Foundation Soils Due to Vertical Subsurfaces Loading. Geotechnique, Nov. 1966.
11. The AASHO Road Test: Report 7—Summary Report. HRB Spec. Rept. 61G, 1962.
12. Larsen, T. J. Tests on Soil-Cement and Cement-Modified Bases in Minnesota. Jour. of PCA Research and Dev. Laboratories, Vol. 9, No. 1, Jan. 1967, pp. 25-47.
13. Larsen, T. J., and Nussbaum, P. J. Fatigue of Soil-Cement. Portland Cement Assn., Bull. D119, 1967.
14. Larsen, T. J., Nussbaum, P. J., and Colley, B. E. Research on Thickness Design for Soil-Cement Pavements. Research and Dev. Laboratories, Portland Cement Assn., Bull. D142, Jan. 1969.
15. Mitchell, J. K., and Freitag, D. R. A Review and Evaluation of Soil-Cement Pavements. Jour. of Soil Mech. and Found. Div., Proc. ASCE, Paper 2294, Dec. 1959.
16. Mitchell, J. K., and Shen, C. K. Soil-Cement Properties Determined by Repeated Loading in Relation to Bases for Flexible Pavements. Proc., Second Internat. Conf. on Structural Design of Asphalt Pavements, Univ. of Michigan, Ann Arbor, 1967.
17. Nussbaum, P. J., and Larsen, T. J. Load-Deflection Characteristics of Soil-Cement Pavements. Highway Research Record 86, 1965, pp. 1-14.
18. Shen, C. K., and Mitchell, J. K. Behavior of Soil-Cement in Repeated Compression and Flexure. Highway Research Record 128, 1966, pp. 68-100.
19. Wang, M. C., Mitchell, J. K., and Monismith, C. L. Behavior of Stabilized Soils Under Repeated Loading: Report 4—Stresses and Deflections in Cement-Stabilized Pavements. Dept. of Civil Eng., Univ. of California, Berkeley, Contract Rept. 3-145, Sept. 1969.
20. Warren, H., and Dieckmann, W. L. Numerical Computation of Stresses and Strains in a Multiple-Layer Asphalt Pavement System. California Research Corp., internal rept., Sept. 1963.
21. Wilson, E. L. Structural Analysis of Axisymmetric Solids. Jour. of American Institute of Aeronautics and Astronautrics, Dec. 1965.

APPENDIX

STRESS AND STRAIN GAGES USED IN TEST PAVEMENTS

Stress Gage

Because the performance of stress gages is directly influenced by soil-gage interaction and because the interaction is a complex function of such factors as the gage dimensions and the gage-to-soil stiffness ratio, it is not feasible to design a gage that can eliminate gage error completely. However, the errors can be minimized by considering the following factors:

1. The thickness-to-diameter ratio should be as small as possible;
2. The ratio of the sensitive area of the gage face to the total facial area should be less than 50 percent;
3. The overall gage stiffness should be as high as possible because the gage cannot be made to always match the soil stiffness (the higher the stiffness is, the better the linearity will be);
4. For measuring stress at a point, the gage size must be small but large enough to minimize effects of nonuniformity of soil texture;
5. For dynamic load purposes, the density of the stress gage must be as close as possible to that of soil to reduce the effect of inertial forces on the stress gage response;
6. Long-term temperature compensation is desirable; and
7. The gage must be waterproof.

For the present investigation, the casing of the gage was made of aluminum alloy 6061-T651, and the strain gage was a full bridge in foil type, catalog No. FAES-4-70-12S13, manufactured by the Baldwin-Lima-Hamilton Corporation. This foil gage was cemented on the diaphragm with BR-610 cement. Details are shown in Figures 19 and 20. The gages were coated with LPS to prevent the reaction of cement with the aluminum casing.

Performance of the stress gages in pavement 1 (3 percent cement) was quite satisfactory. The gages in pavement 2 (6 percent cement), however, did not perform so well, probably because the outputs of the gages in this pavement were too small to be read accurately, even though the diaphragm thickness used in the gages for this pavement was reduced from the 0.45 in. used in pavement 1 to 0.30 in. In pavement 2 the reaction between gage and soil was probably similar to a system composed of a rigid plate overlying a gage that in turn is seated on a soft subgrade soil. The pressure transmitted from the pavement surface in such a system simply pushes the whole gage downward.

All stress gages were first calibrated by using statically applied air pressures, and 2 gages were calibrated in soil having the same characteristics as those of the pavement by using both static and repeated loads. The calibration factors for gages not tested in soil were obtained by assuming that the ratio of calibration factor for static air pressure to that for soil pressure remains constant for all gages having diaphragms of the same thickness.

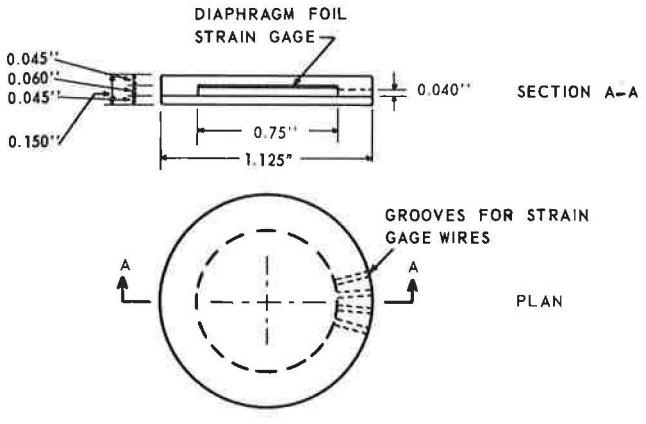

Figure 19. Schematic diagram of stress gage used in test pavements.

A typical calibration curve is shown in Figure 21 for both static and repeated load conditions. The result indicated that static and repeated loads gave almost identical calibrations. A check calibration was made for one gage after the completion of field tests. It was found that calibra-

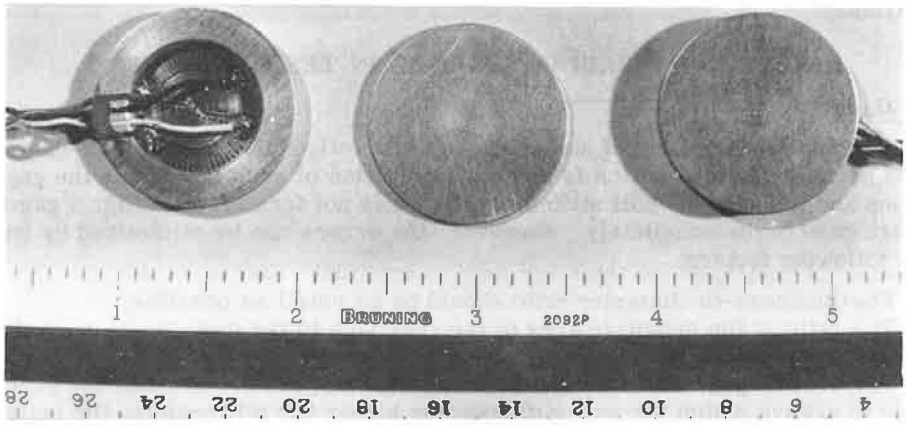

Figure 20. General view of stress gage used in test pavements.

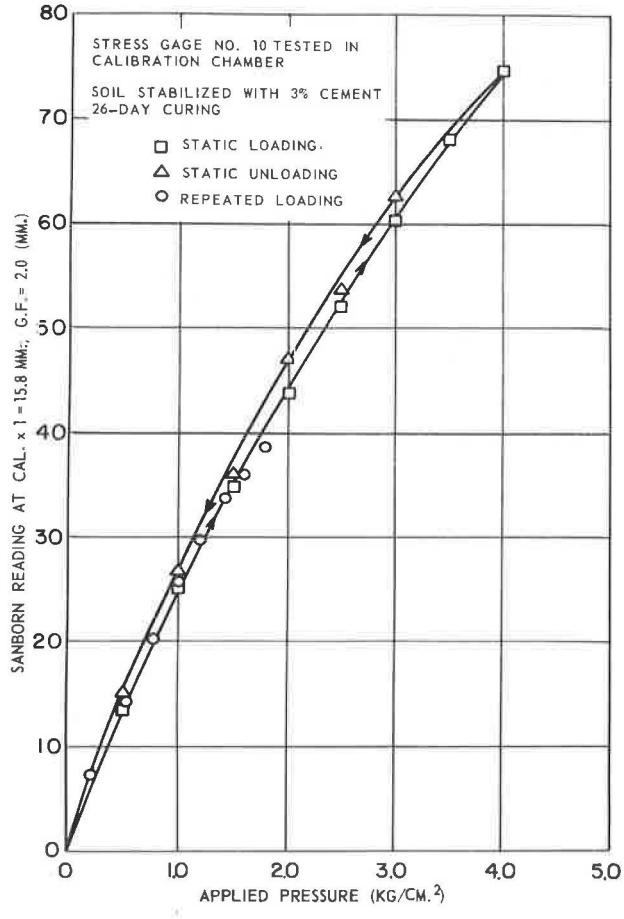

Figure 21. Typical stress gage calibration curve obtained from 20-in. diameter calibration chamber.

tion factor had not changed appreciably after almost 6 months of exposure in the pavement.

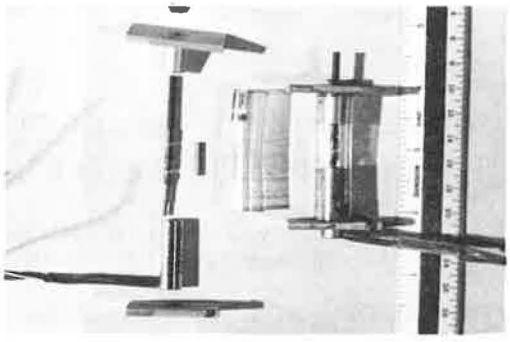

Figure 22. General view of strain gage used in test pavements.

Strain Gage

The strain gage developed for the present study was composed of two $1\frac{1}{2}$-in. by $\frac{3}{4}$-in. by $\frac{1}{8}$-in. aluminum end plates and a single linear variable differential transformer (LVDT) for measuring change in spacing between the plates. The LVDT's used were manufactured by the Sanborn Company, catalog No. 595DT-100. The transformer coil assembly was clamped to one end plate, and the transformer core was screwed on a brass rod that was then fastened to the other end plate. The brass rod had 2 flexible joints so that relative movement of the 2 end plates would not cause friction between the core and coil assembly. A section of $\frac{3}{8}$-in. by 2-in. long polyethylene tubing was used to separate the 2 end plates and to envelop the LVDT to prevent intrusion of soil. Details and a general view of the gage are shown in Figures 22 and 23. All indications were that this type of gage performed very satisfactorily for the measurement of radial strains at the bottom of the stabilized layer.

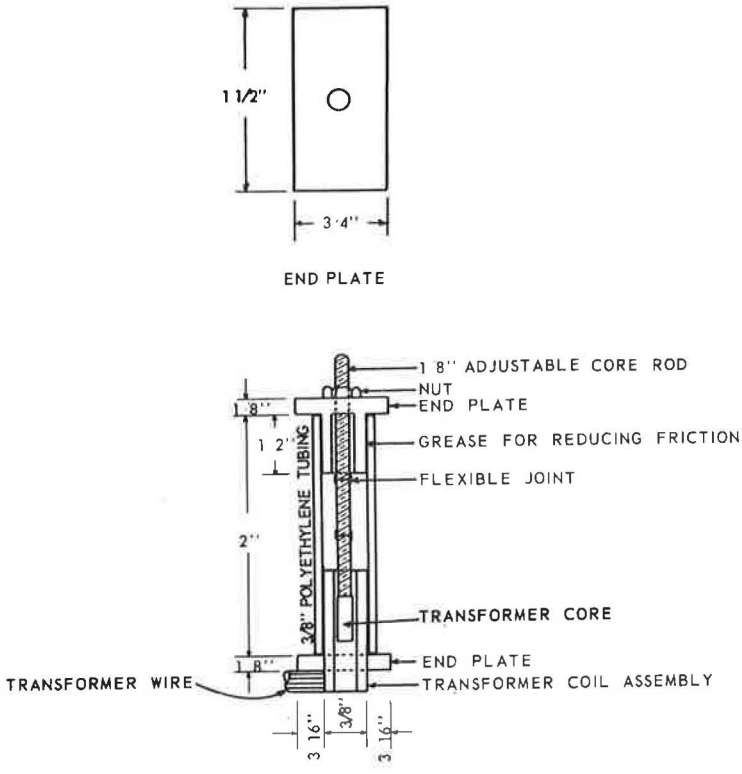

Figure 23. Detailed diagram of strain gage used in test pavements.